Reactivity of Yellow Arsenic towards Cyclic (Alkyl)(Amino) Carbenes (CAACs)

Maria Haimerl, Christoph Schwarzmaier, Christoph Riesinger, Alexey Y Timoshkin, Mohand Melaimi, Guy Bertrand, Manfred Scheer

Chemistry–A European Journal
Research Article
doi.org/10.1002/chem.202300280
Chemistry Europe
European Chemical Societies Publishing
www.chemeurj.org

Reactivity of Yellow Arsenic towards Cyclic (Alkyl)(Amino) Carbenes (CAACs)

Maria Haimerl,[a] Christoph Schwarzmaier,[a] Christoph Riesinger,[a] Alexey Y. Timoshkin,[b] Mohand Melaimi,[c] Guy Bertrand,[c] and Manfred Scheer*[a]

Dedicated to Prof. A. Filippou on the occasion of his 65th birthday.

Abstract: Different cyclic (alkyl)(amino)carbenes (CAACs) were reacted with yellow arsenic. Several products [(CAAC-n)$_2$(μ,$\eta^{1:1}$-As$_2$)] (n = 1 (**1**), 4 (**2**)), [(CAAC-2)$_3$(μ_3,$\eta^{1:1:1}$-As$_4$)] (**3**) and [(CAAC-3)$_4$(μ_4,$\eta^{1:1:1:1}$- As$_8$)] (**6**) were isolated due to the differing steric properties of **CAAC-1-4**. The products contain As$_2$, As$_4$ or As$_8$ units and represent the first examples of CAACs-substituted products of yellow arsenic. The reactivity of As$_4$ was compared with the reactivities of P$_4$ and the interpnictogen compound AsP$_3$, which led to a series of phosphorus-containing derivatives such as ([(CAAC-3)$_3$(μ_3,$\eta^{1:1:1}$-P$_4$)] (**4**) and [(CAAC-3)$_4$(μ_4,$\eta^{1:1:1:1}$-P$_8$)] (**7**)) and [(CAAC-3)$_3$(μ_3,$\eta^{1:1:1}$-AsP$_3$)] (**5**). The products were characterized by spectroscopic and crystallographic methods and DFT computations were performed to clarify their formation pathway.

Introduction

Since their discovery in 2005, cyclic (alkyl)(amino)carbenes (CAACs) have attracted increasing attention and their use as starting materials and co-substituents is a topical field of interest.[1] These carbenes are both more nucleophilic and electrophilic than their NHC counterparts.[2] Their versatile application ranges from coordination chemistry to transition metal catalysis and to the activation of small molecules such as H_2,[3] NH_3,[3] CO[4] and, most interestingly, P_4.[5] Among others, CAACs have the potential to aggregate and fragmentate white phosphorus. In 2007, *Bertrand* et al. reported the first example of a 2,3,4,5-tetraphosphatriene derivative (**A**), stabilized by two menthyl-substituted CAACs (**CAAC-1**,Scheme 1).[6] Depending on the reaction conditions, the reaction of the less sterically protected cyclohexyl-substituted CAAC (**CAAC-2**, Scheme 1) with P_4 leads to three different products: the P_2-dicarbene adduct (**B**),[5a] an isotetraphosphine adduct stabilized by three CAAC molecules (**C**)[5a] and the P_8 tetracarbene compound (**D**)[5b] (Scheme 1). For **D**, a dimerization reaction of two molecules of type **A** was postulated.

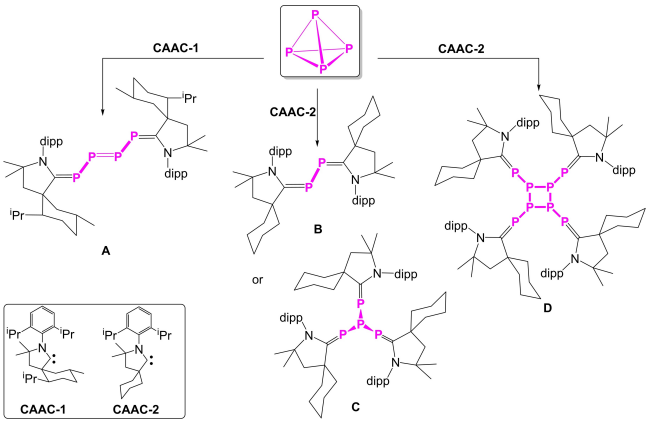

Scheme 1. Conversion of white phosphorus by different CAACs.

While the reactivity of white phosphorus towards transition metal and main group compounds was extensively studied,[7] the related research regarding the conversion of yellow arsenic is limited by its toxicity, light- and air-sensitivity, and the impossibility to carry out stoichiometric reactions due to the autocatalytic conversion to grey arsenic. While there have been several studies of the conversion of yellow arsenic with transition metal complexes containing for example Cp^R or nacnac ligands,[8] there have only been few examples of conversions by main group element compounds.[8–9] Arsenic-arsenic bonds are weaker than phosphorus-phosphorus bonds, which results in less stable intermediates. In the case of yellow arsenic, most likely only the thermodynamically most stable

[a] Dr. M. Haimerl, Dr. C. Schwarzmaier, C. Riesinger, Prof. Dr. M. Scheer
Institute for Inorganic Chemistry
University of Regensburg
Universitätsstraße 31, 93053 Regensburg (Germany)
E-mail: Manfred.scheer@ur.de

[b] Prof. Dr. A. Y. Timoshkin
Institute of Chemistry
St. Petersburg State University
University emb. 7/9, 199034 St. Petersburg (Russia)

[c] Dr. M. Melaimi, Prof. Dr. G. Bertrand
Department of Chemistry and Biochemistry
University of California, San Diego
UCSD-CNRS Joint Research Laboratory (IRL 3555)
La Jolla, CA 92093-0358 (USA)

Supporting information for this article is available on the WWW under https://doi.org/10.1002/chem.202300280

compounds are formed, but there are a few examples of transient species that could be characterized.[9a] Interestingly, there have been efforts to find other ways to prepare arsenic-containing compounds stabilized by CAACs. *Hudnall* et al. synthesized the dicarbene-substituted diarsenic compound [(CAAC-3)$_2$(μ,$\eta^{1:1}$-As$_2$)] (**E**) by reacting **CAAC-3** with AsCl$_3$ and subsequent reduction.[11] There is also one example that has been reported with the heavier analog antimony which is isostructural to [(CAAC-n)$_2$E$_2$] (E = P (**B**), n = 2; As (**E**), n = 3).[12] This product was synthesized by the stepwise reduction of [(CAAC-2)SbCl$_3$] with potassium graphite. Importantly, only a few direct comparisons of P$_4$/As$_4$ reactivity have been reported.[9c,10] For example, the reaction of E$_4$ (E = P, As) with silylene [PhC(N*t*Bu)$_2$SiN(SiMe$_3$)$_2$)] and disilene [(Me$_3$Si)$_2$NCp*Si=SiCp*N(SiMe$_3$)$_2$)] (Cp* = C$_5$Me$_5$) leads to products with different topologies as well as different numbers of substituents and pnictogen atoms.[9c,10c]

Based on the known reaction behavior of CAACs with white phosphorus, the question arose as to whether CAACs could also induce conversions, aggregations, and fragmentations of yellow arsenic as well as to what similarities or differences could be found between the reactivities of P$_4$ and As$_4$.

In contrast to yellow arsenic, the binary isolobal interpnictogen compound AsP$_3$[13] is stable, and can be handled in a way similar to P$_4$. Interestingly, only few examples of the conversion of AsP$_3$ with main group and transition metal compounds have been reported;[14a–e] however, there is a rising interest in nanomaterials containing both phosphorus and arsenic.[14f–h] Therefore, this compound might serve as starting materials for phosphorus-based materials by alloying them with arsenic nuclei. Furthermore, AsP$_3$ might close the gap between white phosphorus and yellow arsenic and, in principle, the reaction behavior of phosphorus and arsenic could be investigated at the same time. With such tools in hand, it is possible to monitor the formation of the products by ^{31}P NMR spectroscopy, which is impossible for yellow arsenic.

Herein, we present a comparative experimental and computational study of the conversion of As$_4$ by different CAACs (**CAAC-1**-**CAAC-4**, Scheme 2). During our investigations, we were also able to synthesize and characterize some new phosphorus containing products and an interpnictogen compound by the reaction of **CAAC-3** with P$_4$ and AsP$_3$, respectively.

Results and Discussion

The reactions of **CAAC-1**, **CAAC-2**, **CAAC-3** and **CAAC-4** with an excess of yellow arsenic in toluene at room temperature led to the formation of the 2,3-diarsabutadiene derivatives [(CAAC-4)$_2$(μ,$\eta^{1:1}$-As$_2$)] (**1**) and [(CAAC-1)$_2$(μ,$\eta^{1:1}$-As$_2$)] (**2**), the isotetraarsine adduct stabilized by three CAAC molecules (**3**) and [(CAAC-3)$_4$(μ_4,$\eta^{1:1:1:1}$-As$_8$)] (**6**) (Scheme 2). The formation of **3** and **6** from the reaction of yellow arsenic with **CAAC-3** is independent of the stoichiometry used. These products are isolated as air-, moisture- and light-sensitive yellow to red crystalline solids in 26% (**1**), 51% (**2**), 21% (**3**), 39% (**6**) yields, respectively (Scheme 2). Changing the reaction conditions (e.g. temperature)[15a] leads to the same products. The reaction between **CAAC-3** and P$_4$ results in the formation of both the isotetraphosphine [(CAAC-3)$_3$(μ_3,$\eta^{1:1:1}$-P$_4$)] (**4**, 54%, see Supporting Information for details) and the P$_8$ tetracarbene derivative [(CAAC-3)$_4$(μ_4,$\eta^{1:1:1:1}$-P$_8$)] (**7**) (Scheme 2). **7** was isolated as crystals in 38% yield. Furthermore, the reaction of AsP$_3$ with **CAAC-3** led to the formation of a yellow air-sensitive crystalline solid. NMR as well as X-ray structural analyses revealed that this solid consists of a mixture of three products, namely [(CAAC-

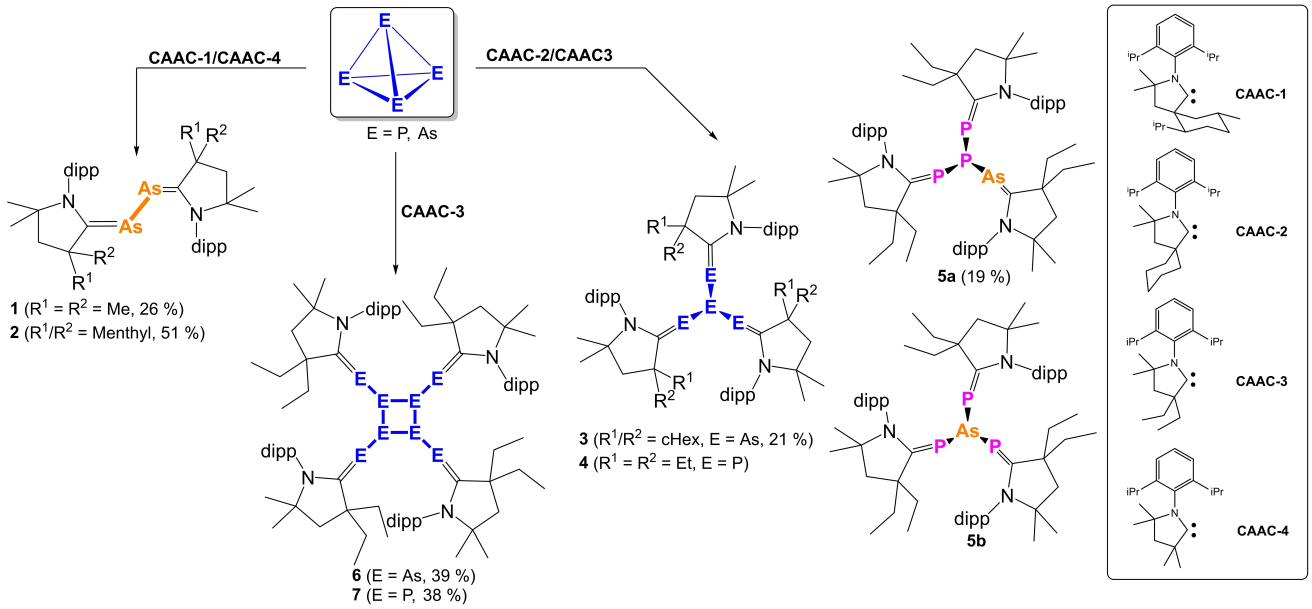

Scheme 2. Conversion of E$_4$ (E$_4$ = P$_4$, As$_4$, AsP$_3$) by different CAACs (dipp = 2,6-diisopropylphenyl). Yields are given in parentheses (those for **5b** and **4** are included in those of **5a**).

3)$_3$(μ_3,$\eta^{1:1:1}$-AsP$_3$)] (**5a**), [(CAAC-3)$_3$(μ_3,$\eta^{1:1:1}$-P$_2$AsP)] (**5b**) and [(CAAC-3)$_3$(μ_3,$\eta^{1:1:1}$-P$_4$)] (**4**) (Scheme 2). In the ^{31}P{^{1}H} NMR spectrum of **5**, a doublet at $\delta = 65.4$ ppm and a triplet at $\delta = -58.9$ ppm ($^1J_{PP} = 242$ Hz) in an integral ratio of 2:1 for the major isomer **5a** and a singlet at $\delta = 74.18$ ppm for the minor isomer **5b** can be detected (there are also signals for **4** visible pointing to a small amount of P$_4$ within an AsP$_3$ sample, see below).

While the reaction of **CAAC-1** with P$_4$ leads to a carbene-stabilized P$_4$ chain (**A**, Scheme 1), the reaction with yellow arsenic results in a carbene-stabilized As$_2$ unit (**2**, Scheme 2). In order to clarify the difference in the reactivity, DFT computations at the B3LYP/def2-SVP level of theory were carried out (see Supporting Information for details). The formation of *trans* isomers of compounds **A**, featuring an E$_4$ chain, is *exergonic* by 81 and 3 kJ mol^{-1} for P and As, respectively. However, the subsequent fragmentation of [(CAAC-1)$_2$E$_4$] (**I-B**, Scheme 3) to [(CAAC-1)$_2$E$_2$] and $^1/_2$ E$_4$ is *endergonic* by 12 kJ mol^{-1} for P, but *exergonic* by 4 kJ mol^{-1} for As. Thus, the P$_4$ chain and the As$_2$ unit are thermodynamically the most favorable products.

Via trapping reactions, *Bertrand* et al. showed that by reacting a CAAC with P$_4$ an unstable monocarbene adduct **I-A** (Scheme 3) is formed as an intermediate.[5b] The formation of this intermediate and the following products (E = P, Scheme 3) were also computationally studied for **CAAC-2** and **CAAC-3** (Scheme 3). Experimentally, the reaction of **CAAC-2** with P$_4$ leads to the formation of **B**, **C** and **D** (Scheme 1). In contrast, the reaction between **CAAC-3** and P$_4$ leads to **4** and **7**. In the case of arsenic, the formation of other products during the reaction cannot be precluded but is hard to monitor due to the poor NMR features of arsenic compounds. For the formation of **6** and **7**, two different reaction pathways can be proposed (Scheme 3). The first one includes the formation of the **I-B** intermediate which is exergonic both for P and As (Scheme 3). The subsequent dimerization of two molecules of **I-B** to **6** and **7** is also exergonic by 93 and 121 kJ mol^{-1}, respectively. The second pathway includes the formation of **I-A** as the first step and, afterwards, a direct formation of **6** and **7** or an indirect route via **I-B** (Scheme 3). By changing the stoichiometry, it was also possible to synthesize **4**, but not its arsenic analog [(CAAC-3)$_3$As$_4$]. [(CAAC-3)$_3$E$_4$] is expected to be built via an **I-A** intermediate. Since the **I-A** formation is slightly *endergonic* for As, this reaction pathway would be less favorable than the formation of **6** via an **I-B** intermediate. This could explain the sole formation of **6** in the case of the reaction with As$_4$.

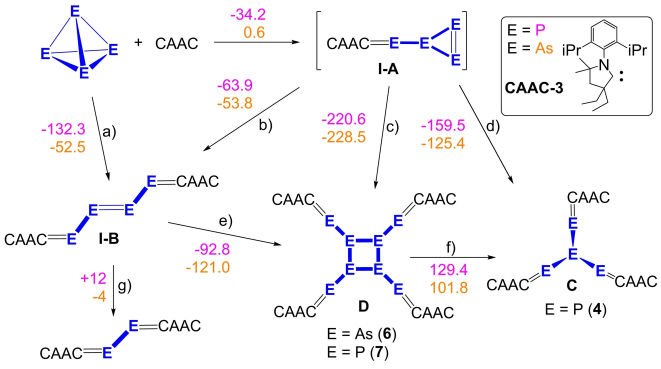

Scheme 3. Standard Gibbs energies for the suggested reaction pathways (ΔG°_{298} values are in kJ mol^{-1} for **CAAC-3**, values for **CAAC-2** see Supporting Information). a) + 2 CAAC; b) 2x **I-A**, − P$_4$; c) 4x **I-A**, −2 P$_4$; d) + 2 CAAC; e) 2x **I-B**; f) for the reaction **D** = **C** + **I-A**; g) values for **CAAC-1**, −1/2 E$_4$.

The ^{1}H NMR spectra of **1**, **6** and **7** reveal a high symmetry with one set of signals for the CAAC units. The ^{31}P{^{1}H} NMR spectrum of **4** in C$_6$D$_6$ at room temperature reveals a doublet at $\delta = 69.9$ ppm ($^1J_{PP} = 236$ Hz) and a quartet at $\delta = -57.6$ ppm ($^1J_{PP} = 236$ Hz), matching the AM$_3$ pattern expected for **C**. In the case of **5**, two isomers are visible in the ^{31}P{^{1}H} NMR spectrum indicating a different chemical and magnetic environment, which can be explained by the position of the arsenic atom. Which isomer is formed, depends on the subsequent bond cleavage within the AsP$_3$ tetrahedron by the carbene. The bond cleavage of an As–P bond in AsP$_3$ is by 6 kJ mol^{-1} less energy-demanding than a P–P bond cleavage.[14d] Two As–P and one P–P bond cleavages lead to the formation of the major isomer **5a** with the carbene-coordinated arsenic atom (Scheme 2). Three P–P bond cleavages of the AsP$_3$ tetrahedron lead to the minor isomer **5b**, where the arsenic atom is in the middle of the E$_4$ unit (Scheme 2). Furthermore, the ^{31}P{^{1}H} NMR spectrum of **7** shows two multiplets at $\delta = 52.7$ ppm and −54.9 ppm (comparable to **D**). In the LIFDI-MS spectra of **1**, **2**, **5** and **7**, respectively, the corresponding molecular ion peaks are detected. Compound **3** is visible in traces in the LIFDI-MS spectrum and, for **6**, the LIFDI-MS spectrum shows different fragments of ((CAAC-3)$_3$As$_7$), (CAAC-3)$_2$As$_n$) (n = 2, 3, 5)), but not the molecular ion peak, which emphasizes the high sensitivity of arsenic-rich compounds.

For **2**, cyclic voltammetry measurements in THF were performed (cf. Supporting Information). Compound **2** reveals a first reversible oxidation at −658 mV and a second irreversible oxidation at −350 mV (against [Cp$_2$Fe]/[Cp$_2$Fe]$^+$). Compared to the corresponding phosphorus analogs of **2**, **B** shows a reversible oxidation at −536 mV.[15b] Thus, **2** can more easily be oxidized. This could be explained by the resonance form **II** shown in Scheme 4. Due to arsenic being less prone to form double bonds, the canonical form (**I**) might be less important than form (**II**) which contains an electron-rich As$_2$ unit.

The molecular structures of **1** and **2** reveal a central As$_2$ unit binding in $\eta^{1:1}$ fashion to two CAAC fragments (Figure 1). The C2-As1-As2-C21/C28 dihedral angle amounts to 175.6(1)° (**1**) and 165.7(1)° (**2**), respectively. Furthermore, the carbene carbon

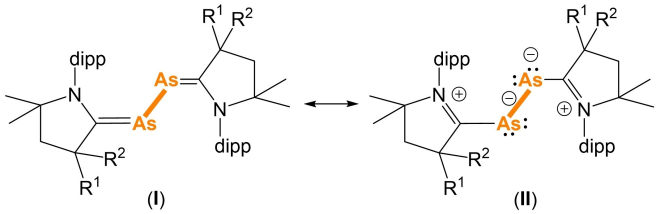

Scheme 4. Canonical forms of 2,3-diarsabutadiene (**I**) and a charge-separated diarsinediid (**II**).

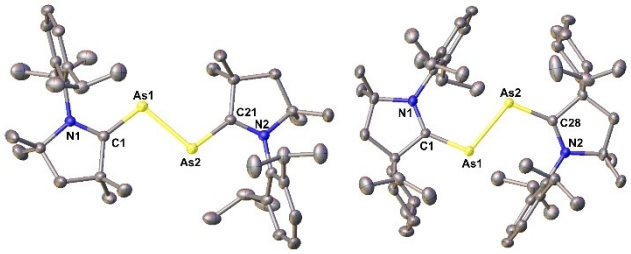

Figure 1. Molecular structures of **1** (left) and **2** (right) in the solid state. Thermal ellipsoids are shown at 50% probability level. Hydrogen atoms are omitted for clarity.

atoms reveal a typical planar geometry for sp^2-hybridized carbon atoms (sum of angles; **1**: 360° for C1 and C21; **2**: 359.8° for C1 and 359.9° for C28). While in **1** the diisopropylphenyl groups of the CAAC groups point away from the As_2 unit, they point towards the As_2 unit in **2**. This could be explained by the steric effect of the bulky menthyl group being larger than the one of the diisopropylphenyl groups in **2** (buried volume for **CAAC-1**: 77.4%, for **CAAC-4**: 71.9%).[16] The As1-As2 bond distance amounts to 2.4175(2) Å (**1**) and 2.4423(4) (**2**) Å, respectively, which is in the typical range of an As–As single bond (determined by electron diffraction:[17] 2.435(4) Å, by DFT computations:[18] 2.437 Å, by the sum of covalent radii:[19] 2.42 Å). The C–As bond distances are halfway between a single[19] and a double bond[20] (**1**: 1.8520(14) and 1.8528(14) Å; **2**: 1.856(3) and 1.859(3) Å). The C1–N1 and C21/C28–N2 bond distances with 1.3645(17) Å and 1.3621(17) Å for **1**, 1.371(4) Å and 1.364(4) Å for **2**, respectively, are slightly shorter than the corresponding C–N bond distances in **B** (1.387(9) Å).[5a]

The molecular structures of **3** and **5** reveal an iso-tetrapnictogen unit (E = As (**3**), AsP_3 (**5**)) that is stabilized by

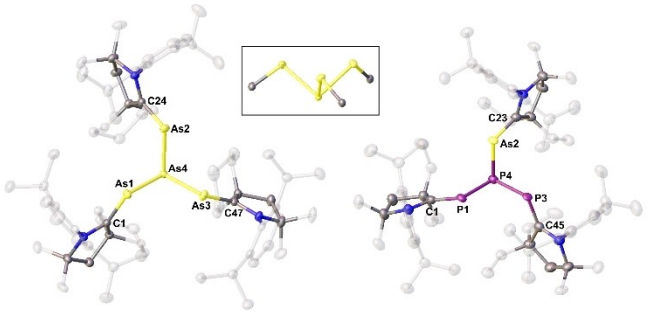

Figure 2. Molecular structure of **3** (left) and **5a** (right, one isomer of **5**) in the solid state, side view of the E_4 unit (box). Thermal ellipsoids are shown at 50% probability level. Hydrogen atoms and solvent molecules are omitted for clarity.

Table 1. Occupation of the phosphorus and arsenic positions in compound **5**.

Atom	1	2	3	4
P	70	76	75	95
As	30	24	25	5

three CAAC substituents (Figure 2). The arsenic atom in **5** is disordered over all four pnictogen positions (Table 1). The major isomer **5a** with the carbene-coordinated arsenic atom as well as the minor isomer **5b** with the arsenic atom at position E4 are found to be in a ratio of 79:5 (16% corresponds to compound **4**) in the solid state (Scheme 2). DFT computations indicate that, in the gas phase, the standard Gibbs energy for the equilibrium **5a** to **5b** is exergonic by 22.1 kJ mol^{-1}, indicating that isomer **5b** is the thermodynamically stable product (see Supporting Information). The higher amount of **5a** in the experiment is most likely due to kinetic reasons. To understand the formation of both isomers, the energy associated with the initial reaction between **CAAC3** and AsP_3 was calculated. We found that the attack of the carbene at a P atom is more exergonic by 24.6 kJ mol^{-1} than the attack at the As atom. The breaking of the P–As bond in the (CAAC-3)$PAsP_2$ intermediate is expected to proceed more easily than that in the P–P bond, resulting in **5a** rather than in **5b**. The formation of **4** upon reaction with AsP_3 can be explained by the thermodynamic favorability of the disproportionation of AsP_3: 4 AsP_3 = 3 P_4 + As_4 (computed gas phase $\Delta G°_{298}$ = -13.6 kJ mol^{-1}). The formed As_4 can isomerize into unreactive grey arsenic and quit the reaction.

The angles around the central atom E4 are in the range of 89.28(1)° to 92.24(1)° for **3**, 86.81(1)° to 92.88(1)° for **5a** and 86.54(1)° to 86.99(1)° for **5b**. In comparison to **C** which has all three angles at 90.15(2)°, **3** and **5** show more deviation from the perfect local C_{3v} symmetry. In both structures, the diisopropylphenyl groups of the CAAC substituents point away from the central atom E4, and the CAAC fragments themselves are bent counter clockwise in the case of **3** and clockwise in the case of **5** (**C**: clockwise). In the case of arsenic, the CAAC fragments are bent in the opposite direction than in the case of phosphorus. Interestingly, the CAAC units in the mixed interpnictogen compound **5** and in the phosphorus analogue **C** have the same orientation. The As–As bond distances of **3** are in between 2.4479(2) and 2.4520(2) Å which is in the range of an arsenic single bond.[19] The E–E bond distances of **5** are in the range of normal single bonds (P–P: 2.212(10) to 2.263(8) Å, P–As: 2.289(11) to 2.40(4) Å). The C–E bond distances are in between a single and a double bond (**3**: 1.862(2) to 1.866(2) Å; **5**: C–P: 1.714(8) to 1.748(10) Å, C–As: 1.856(9) to 1.891(10) Å).

The molecular structure of **6** and **7** (Figure 3) reveals a tetra(carbene)E_8 cage compound (E = As (**6**), P (**7**)) which contains a four-membered E_4 ring with each pnictogen atom being connected to a further pnictogen atom and stabilized by four CAAC fragments. For the phosphorus compound **7**, the P_4 cycle is nearly planar (torsion angle: 171.8°) possessing almost right angles (P2-P3-P2' 89.70(3)° and P3-P2-P3' 90.01(3)°), which is in contrast to the reported compound **D** that has a similar structural P_8 motif, with the P_4 cycle, however, being folded by 47.90°. In compound **6**, the As_4 cycle is folded by 55.54° (As1-As2-As3 plane: As2-As3-As4 plane). The diisopropylphenyl groups of both compounds point away from the E_8 unit. The E–E–C angels are very similar for both compounds (**6**: 102.71(9) - 104.05(10)°; **7**: 101.01(4)/104.66(7)°). So here the main difference is the inner E_4 cycle. The E–E bond distances in the *cyclo*-E_4 unit are between 2.4538(5) and 2.4741(5) Å (**6**),

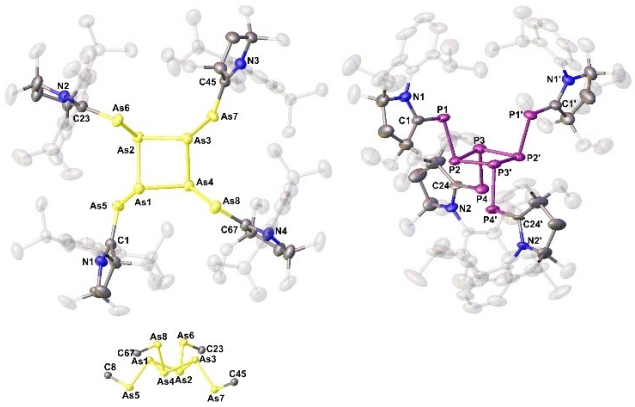

Figure 3. Molecular structures of **6** (left) and **7** (right) in the solid state (bottom: side view of the As_8 unit). Thermal ellipsoids are shown at 50% probability level. Hydrogen atoms are omitted for clarity.

2.2335(8) and 2.2354(8) Å (**7**), respectively, representing elongated single bonds. The other E–E bond distances are in the range of ordinary single bonds (**6**: 2.4237(5)–2.4334(5) Å, **7**: 2.1975(7) and 2.1987(7) Å). The C–E bond distances of **6** (between 1.862(3) and 1.864(3) Å) and **7** (1.731(2), 1.797(13) Å) are also halfway between a single and a double bond.

Conclusion

First investigations of the reactivity of yellow arsenic towards carbenes are presented. This work demonstrates that the reaction of yellow arsenic with CAACs leads to aggregation, fragmentation, and rearrangement of As_4. The reaction outcome depends on the sterics of the respective CAAC. By reacting different CAACs with As_4, the compounds $[(CAAC\text{-}4)_2(\mu,\eta^{1:1}\text{-}As_2)]$ (**1**), $[(CAAC\text{-}1)_2(\mu,\eta^{1:1}\text{-}As_2)]$ (**2**), $[(CAAC\text{-}2)_3(\mu_3,\eta^{1:1:1}\text{-}As_4)]$ (**3**) and $[(CAAC\text{-}3)_4(\mu_4,\eta^{1:1:1:1}\text{-}As_8)]$ (**6**) were obtained. These products represent the first examples of polyarsenic units containing CAACs entities. By conversion of yellow arsenic with CAACs, only the thermodynamically most stable products could be isolated. These products are less stable than their phosphorus analogues, which also affects the isolated yields. DFT computations are in qualitative agreement with the experimental observations. Furthermore, the products $[(CAAC\text{-}3)_3(\mu_3,\eta^{1:1:1}\text{-}P_4)]$ (**4**), $[(CAAC\text{-}3)_4(\mu_4,\eta^{1:1:1:1}\text{-}P_8)]$ (**7**) and $[(CAAC\text{-}3)_3(\mu_3,\eta^{1:1:1}\text{-}AsP_3)]$ (**5**) were synthesized. The latter represents the first product of the reactivity of AsP_3 towards CAACs. Moreover, the different reaction outcomes and structural differences of the reactions with white phosphorus, yellow arsenic and the interpnictogen compound AsP_3 were discussed, most reflected by the instability of kinetically formed products and their subsequent reactions in case of the As_4 reactions. Furthermore, the use of AsP_3 might open a new modification strategy for phosphorus-based materials doped with arsenic.

Experimental Section

Experimental procedures for the synthesis of all compounds, analytical data, quantum chemical calculations and X-ray crystallography are described in the Supporting Information.

Deposition Number(s) 2205186 (for **1**), 2205187 (for **2**), 2205188 (for **3**), 2205189 (for **5**), 2205190 (for **6**) and 2205191 (for **7**) contain(s) the supplementary crystallographic data for this paper. These data are provided free of charge by the joint Cambridge Crystallographic Data Centre and Fachinformationszentrum Karlsruhe Access Structures service.

Acknowledgements

This work was supported by the Deutsche Forschungsgemeinschaft within the project Sch 384/40-1, and by the U.S. Department of Energy, Office of Science, Basic Energy Sciences, Catalysis Science Program, under Award No. DE-SC0009376. C. R. is grateful to the Studienstiftung des deutschen Volkes e. V. for a PhD fellowship. Open Access funding enabled and organized by Projekt DEAL.

Conflict of Interests

The authors declare no conflict of interest.

Data Availability Statement

The data that support the findings of this study are available in the supplementary material of this article.

Keywords: CAAC · interpnictogen compound · polyarsenic compounds · yellow arsenic

[1] V. Lavallo, Y. Canac, C. Präsang, B. Donnadieu, G. Bertrand, *Angew. Chem. Int. Ed.* **2005**, *44*, 5705–5709; *Angew. Chem.* **2005**, *117*, 5851–5855.
[2] a) M. Soleilhavoup, G. Bertrand, *Acc. Chem. Res.* **2015**, *48*, 256–266; b) S. Roy, K. C. Mondal, H. W. Roesky, *Acc. Chem. Res.* **2016**, *49*, 357–369; c) M. Melaimi, M. Soleilhavoup, G. Bertrand, *Angew. Chem. Int. Ed.* **2010**, *49*, 8810–8849; *Angew. Chem.* **2010**, *122*, 8992–9032; d) T. Dröge, F. Glorius, *Angew. Chem. Int. Ed.* **2010**, *49*, 6940–6952; *Angew. Chem.* **2010**, *122*, 7094–7107; e) D. Martin, M. Melaimi, M. Soleilhavoup, G. Bertrand, *Organometallics* **2011**, *30*, 5304–5313; f) F. E. Hahn, M. C. Jahnke, *Angew. Chem. Int. Ed.* **2008**, *47*, 3122–3172; *Angew. Chem.* **2008**, *120*, 3166–3216; g) S. Würtemberger-Pietsch, U. Radius, T. B. Marder, *Dalton Trans.* **2016**, *45*, 5880–5895; h) M. Melaimi, R. Jazzar, M. Soleilhavoup, G. Bertrand, *Angew. Chem. Int. Ed.* **2017**, *56*, 10046–10068; *Angew. Chem.* **2017**, *129*, 10180–10203; i) R. Jazzar, M. Soleilhavoup, G. Bertrand, *Chem. Rev.* **2020**, *120*, 4141–4168; j) M. R. Serrato, M. Melaimi, G. Bertrand, *Chem. Commun.* **2022**, *58*, 7519–7521.
[3] G. D. Frey, V. Lavallo, B. Donnadieu, W. W. Schoeller, G. Bertrand, *Science* **2007**, *316*, 439–441.
[4] V. Lavallo, Y. Canac, B. Donnadieu, W. W. Schoeller, G. Bertrand, *Angew. Chem. Int. Ed.* **2006**, *45*, 3488–3491; *Angew. Chem.* **2006**, *118*, 3568–3571.
[5] a) O. Back, G. Kuchenbeiser, B. Donnadieu, G. Bertrand, *Angew. Chem. Int. Ed.* **2009**, *48*, 5530–5533; *Angew. Chem.* **2009**, *121*, 5638–5641; b) C. D. Martin, C. M. Weinstein, C. E. Moore, A. L. Rheingold, G. Bertrand, *Chem. Commun.* **2013**, *49*, 4486–4488.

[6] J. D. Masuda, W. W. Schoeller, B. Donnadieu, G. Bertrand, *Angew. Chem.* **2007**, *119*, 7182–7185; *Angew. Chem. Int. Ed.* **2007**, *46*, 7052–7055.
[7] a) O. J. Scherer, *Angew. Chem. Int. Ed. Engl.* **1985**, *24*, 924–943; b) O. J. Scherer, *Angew. Chem. Int. Ed. Engl.* **1990**, *29*, 1104–1122; c) M. Scheer, E. Herrmann, *Z. Chem.* **1990**, *30*, 41–55; d) B. Rink, O. J. Scherer, G. Heckmann, G. Wolmershauser, *Chem. Ber.* **1992**, *125*, 1011–1016; e) O. J. Scherer, *Acc. Chem. Res.* **1999**, *32*, 751–762; f) O. J. Scherer, *Chem. Unserer Zeit* **2000**, *34*, 374–381; g) M. Peruzzini, L. Gonsalvi, A. Romerosa, *Chem. Soc. Rev.* **2005**, *34*, 1038–1047; h) B. M. Cossairt, N. A. Piro, C. C. Cummins, *Chem. Rev.* **2010**, *110*, 4164–4177; i) M. Scheer, G. Balázs, A. Seitz, *Chem. Rev.* **2010**, *110*, 4236–4256; j) N. A. Giffin, J. D. Masuda, *Coord. Chem. Rev.* **2011**, *255*, 1342–1359; k) S. Khan, S. S. Sen, H. W. Roesky, *Chem. Commun.* **2012**, *48*, 2169–2179; l) M. H. Holthausen, J. J. Weigand, *Chem. Soc. Rev.* **2014**, *43*, 6639–6657; m) C. M. Hoidn, D. J. Scott, R. Wolf, *Chem. Eur. J.* **2021**, *27*, 1886–1902.
[8] M. Seidl, G. Balázs, M. Scheer, *Chem. Rev.* **2019**, *119*, 8406–8434.
[9] a) R. P. Tan, N. M. Comerlato, D. R. Powell, R. West, *Angew. Chem. Int. Ed. Engl.* **1992**, *31*, 1217–1218; b) S. Heinl, G. Balázs, A. Stauber, M. Scheer, *Angew. Chem. Int. Ed.* **2016**, *55*, 15524–15527; *Angew. Chem.* **2016**, *128*, 15751–15755; c) A. E. Seitz, M. Eckhardt, S. S. Sen, A. Erlebach, E. V. Peresypkina, H. W. Roesky, M. Sierka, M. Scheer, *Angew. Chem. Int. Ed.* **2017**, *56*, 6655–6659; *Angew. Chem.* **2017**, *129*, 6755–6759.
[10] a) F. Spitzer, G. Balázs, C. Graßl, M. Keilwerth, K. Meyer, M. Scheer, *Angew. Chem. Int. Ed.* **2018**, *57*, 8760–8764; *Angew. Chem.* **2018**, *130*, 8896–8900; b) F. Spitzer, C. Graßl, G. Balázs, E. Mädl, M. Keilwerth, E. M. Zolnhofer, K. Meyer, M. Scheer, *Chem. Eur. J.* **2017**, *23*, 2716–2721; c) S. Khan, R. Michel, S. S. Sen, H. W. Roesky, D. Stalke, *Angew. Chem. Int. Ed.* **2011**, *50*, 11786–11789; *Angew. Chem.* **2011**, *123*, 11990–11993; d) M. Schmidt, D. Konieczny, E. V. Peresypkina, A. V. Virovets, G. Balázs, M. Bodensteiner, F. Riedlberger, H. Krauss, M. Scheer, *Angew. Chem. Int. Ed.* **2017**, *56*, 7307–7311; *Angew. Chem.* **2017**, *129*, 7413–7417; e) M. V. Butovskiy, G. Balázs, M. Bodensteiner, E. V. Peresypkina, A. V. Virovets, J. Sutter, M. Scheer, *Angew. Chem. Int. Ed.* **2013**, *52*, 2972–2976; *Angew. Chem.* **2013**, *125*, 3045–3049; f) M. Piesch, C. Graßl, M. Scheer, *Angew. Chem. Int. Ed.* **2020**, *59*, 7154–7160; *Angew. Chem.* **2020**, *132*, 7220–7227.
[11] K. M. Melancon, M. B. Gildner, T. W. Hudnall, *Chem. Eur. J.* **2018**, *24*, 9264–9268.
[12] R. Kretschmer, D. A. Ruiz, C. E. Moore, A. L. Rheingold, G. Bertrand, *Angew. Chem. Int. Ed.* **2014**, *53*, 8176–8179; *Angew. Chem.* **2014**, *126*, 8315–8318.
[13] a) B. M. Cossairt, M.-C. Diawara, C. C. Cummins, *Science* **2009**, *323*, 602–602; b) B. M. Cossairt, C. C. Cummins, A. R. Head, D. L. Lichtenberger, R. J. F. Berger, S. A. Hayes, N. W. Mitzel, G. Wu, *J. Am. Chem. Soc.* **2010**, *132*, 8459–8465.
[14] a) B. M. Cossairt, C. C. Cummins, *J. Am. Chem. Soc.* **2009**, *131*, 15501–15511; b) B. M. Cossairt, C. C. Cummins, *Chem. Eur. J.* **2010**, *16*, 12603–12608; c) C. Schwarzmaier, A. Noor, G. Glatz, M. Zabel, A. Y. Timoshkin, B. M. Cossairt, C. C. Cummins, R. Kempe, M. Scheer, *Angew. Chem. Int. Ed.* **2011**, *50*, 7283–7286; *Angew. Chem.* **2011**, *123*, 7421–7424; d) T. A. Engesser, W. J. Transue, P. Weis, C. C. Cummins, I. Krossing, *Eur. J. Inorg. Chem.* **2019**, *2019*, 2607–2612; e) M. Haimerl, M. Piesch, R. Yadav, P. W. Roesky, M. Scheer, *Chem. Eur. J.* **2023**, *29*, e202202529; f) M. R. Molas, Ł. Macewicz, A. Wieloszyńska, P. Jakóbczyk, A. Wysmołek, R. Bogdanowicz, J. B. Jasinski, *NPJ 2D Mater. Appl.* **2021**, *5*, 1–24; g) Y. Hu, J. Liang, Y. Xia, C. Zhao, M. Jiang, J. Ma, Zuoxiu Tie, Z. Jin, *Small* **2022**, *18*, 2104556; h) J. Liang, Y. Hu, K. Zhang, Y. Wang, X. Song, A. Tao, Y. Liu, Z. Jin, *Nano Res.* **2022**, *15*, 3737–3752.
[15] a) Note: low temperature reactions were not possible due to the bad solubility of As_4 below r.t; b) O. Back, B. Donnadieu, P. Parameswaran, G. Frenking, G. Bertrand, *Nat. Chem.* **2010**, *2*, 369–373.
[16] L. Falivene, Z. Cao, A. Petta, L. Serra, A. Poater, R. Oliva, V. Scarano, L. Cavallo, *Nat. Chem.* **2019**, *11*, 872–879.
[17] Y. Morino, T. Ukaji, T. Ito, *Bull. Chem. Soc. Jpn.* **1966**, *39*, 64–71.
[18] H. A. Spinney, N. A. Piro, C. C. Cummins, *J. Am. Chem. Soc.* **2009**, *131*, 16233–16243.
[19] P. Pyykkö, M. Atsumi, *Chem. Eur. J.* **2008**, *15*, 186–197.
[20] P. Pyykkö, M. Atsumi, *Chem. Eur. J.* **2009**, *15*, 12770–12779.

Manuscript received: January 27, 2023
Accepted manuscript online: April 4, 2023
Version of record online: May 2, 2023